EFFECT OF ECCENTRICITY ON THE PRESSURE AND VELOCITY GRADIENTS ALONG A STREAMLINE PAST A CYLINDERICAL BODY

Ali A. Jazie Al-Khaledy
College of engineering
Al-Qadisiya University

Abstract

In chemical technology and power engineering, equipment containing heat exchanging pipes and various cylindrical links immersed into moving fluid was often used. The estimation of the hydrodynamic action on these elements is based on the solution of the plane problem on the flow past a cylinder. In the hydrodynamics of inviscid flow past a body of nonzero thickness, it was assumed that there are regions near the body in which the flow accelerates from the front stagnation point to the midsection and decelerates behind the midsection. According to the Bernoulli theorem, a pressure counter-gradient arises in the deceleration region, which acts both in the outer flow and in the boundary layer. For the inviscid flow, the fluid particles store sufficiently much kinetic energy in the acceleration region to overcome this barrier, but in the frictional flow, the fluid particles that remain in the boundary layer cannot reach the region of higher pressure. They are pushed away from the wall, and an opposite flow arises downstream. This phenomenon is known as the boundary layer separation. A CFD models were simulated for the viscous flow past bodies changed from a circular cylinder to flat plate. FLUENT 6.3.26 package was used for solving the model preprocessed in GAMBIT 2.3.16 for flow past a body. Fluent solvers were based on the finite volume method and general conservation (transport) equation for momentum was discretized into algebraic equations. The pressure and velocity gradients for viscous flow past bodies changed from a circular cylinder to flat plate was predicted and plotted and the effect of eccentricity on the pressure and velocity gradients was studied.

Key words: viscous flow, aspect ratio, boundary layer separation, wake, bluff body

تأثير معامل المركزية على تدرج السرعة والضغط على طول خطوط الجريان حول جسم اسطواني

علي عبد الحسين جازع
ماجستير هندسة كيمياوية
كلية الهندسة جامعة القادسية

الخلاصة

في الهندسة الكيمياوية وهندسة الطاقة ، عادة تستخدم المعدات التي تحتوي على أنابيب التبادل الحراري و الاسطوانات المختلفة المغمورة داخل مائع متحرك.حساب التأثير الهيدروديناميكي على هذه العناصر معتمد على حل مسالة الجريان حول اسطوانة في هيدروديناميكية الموائع الغير لزجة (inviscid flow) حول جسم ذو سمك لايساوي صفر يفترض بان هنالك مناطق. بالقرب من الجسم فيها الجريان يعجل من نقطة الركود الى منتصف المقطع ثم يثبط بعد منصف المقطع .طبقا الى نظرية برنولي ،تدرج ضغط ينشا في هذه المنطقة والذي يؤثر على كلا الجريان الخارجي والطبقة المتاخمة. بالنسبة للجريان الغير لزج ،جسيمات المائع تختزن كمية كافية من الطاقة الحركية في منطقة التعجيل لتتغلب على ذلك ولكن في الجريان الاحتكاكي ،جسيمات المائع الباقية في الطبقة المتاخمة لايمكن ان تصل الى منطقة الضغط العالي .هذه الجسيمات يتم دفعها بعيدا عن الجدار وهنا ينشا جريان باتجاه معاكس .هذه الظاهرة تعرف بمصطلح انفصال الطبقة المتاخمة. في هذا البحث تم استخدام (CFD models) لجريان لزج حول جسم اسطواني متغير الشكل للمقطع من اسطوانة دائرية الى صفيحة مستوية.تم استخدام برنامج (FLUENT 6.3.26) لحل الموديل المعالج مسبقا باستخدام(GAMBIT 2.3.16) للجريان حول جسم اسطواني .برنامج (FLUENT 6.3.26)معتمد على طريقة الحجم المحدد ومعادلات الحفظ العامة للكتلة والزخم والطاقة والتي يتم تجزئتها الى معادلات جبرية . في هذا البحث تم تحري كيفية تغير تدرج السرعة والضغط بالنسبة لجريان لزج حول اجسام متغيرة الشكل بدءا بالاسطوانة الدائرية وانتهاء بالصفيحة المستوية وتم رسم النتائج وبيان تاثير تغير الشكل على تدرج السرعة والضغط.

Introduction

The flow around circular cylinders has been studied with experimental, analytical and numerical techniques (Coutanceau and Bouard, 1977). However, there is a paucity of experimental and computational data for flow around ellipses at low Reynolds numbers that is due, at least in part, to the economic imperatives for studying higher Reynolds number flows that are common for vehicles and machinery. However, microfluidics research is now becoming recognized as a field in its own right (D. Li, 2004). When using inviscid models, the flow pattern is symmetrical not only above and below the cylinder, but also upstream and downstream. However, for viscous flows above Reynolds numbers of approximately one, dynamic forces override the fore and aft symmetry. As the flow rate increases, a separation appear on the downstream side that contains two recirculating eddies that grow laterally as the Reynolds number increases. In the mid 19th century, Stokes developed an analytical description of flow past a motionless sphere at Reynolds numbers less than 1. Oseen extended Stokes's work to cylinders using an analysis based upon slight deviations from a known flow (Streeter,1961). Schlichting reported on the work by Blasius and others in the early 1900s to develop exact solutions for flow around simple shapes (Schlichting,1979). The velocity of the potential flow and the velocity profile of the boundary layer were expressed as power series in x, the distance from the stagnation point measured along the object's contour. Lack of sufficient computational resources to include an adequate number of terms limited the accuracy of the calculations, especially for slender body shapes such as streamlined ellipses. Taneda experimented with circular cylinders and flat plates aligned parallel to the flow for Reynolds numbers in the range 1–2000 (Taneda, 1956). He observed the formation of twin rear

vortices behind a circular cylinder at a Reynolds number of 7. He later extended his work by taking detailed measurements of the recirculating eddies behind flat plates oriented normal to the flow (Taneda,1968). He found measurable eddies at a Reynolds number of 0.92. He also measured the relationship between the eddy size and Reynolds number. Dennis and Chang presented finite difference solutions of the equations of motion for steady, incompressible flow around a circular cylinder for Reynolds numbers in the range 5–100 (Dennis and Chang, 1970). Like Taneda (Taneda, 1956) they found a linear growth in eddy length with increasing Reynolds number behind a circular cylinder. They calculated that flow separation begins at a critical Reynolds number of 6.2. Nieuwstadt and Keller modeled viscous flow around a circular cylinder for Reynolds numbers in the range 1–40 using the semi-analytical method of series truncation to express the stream function and vorticity in a Fourier series that was substituted into the Navier–Stokes equation to yield a finite system of nonlinear ordinary differential equations (Nieuwstadt and Keller, 1973). Their results compared favorably with Dennis and Chang (Dennis and Chang,1970) for Reynolds numbers less than 40, and were computationally more efficient.

Coutanceau and Bouard photographed features of wakes behind circular cylinders for Reynolds numbers in the range of 5–40 (Coutanceau and Bouard,1977). They noted that the maximum recirculating velocity on the axis between the eddies increased linearly with Reynolds number. Van Dyke published experimental visualizations of flow around circular cylinders at Reynolds numbers of 0.16 and 1.54 (Van Dyke,1983). In the former case, the flow was almost completely symmetrical upstream and downstream of the object. In the latter case, the streamlines downstream of the cylinder were elongated, but the flow was not separated. He also published Taneda's photograph (Taneda,1968) of flow past a flat plate normal to the flow at a Reynolds number of 0.334. Although Taneda did not claim flow separation for this case, Van Dyke entertained the possibility. Shintani, Umemura and Takano asymptotically matched the Stokes and Oseen solutions of the Navier–Stokes equations for two overlapping regions near elliptic cylinders at a Reynolds number of 0.1 (Shintani et al , 1983). For a flat plate, two symmetrical recirculating vortices formed on the downstream side. They reported qualitative agreement with Taneda's illustration (S. Taneda, 1968) of flow at a Reynolds number of 0.44. Nakayama et al. presented visualizations of flows around a circular cylinder at Reynolds numbers of 0.038 and 1.1 (Nakayama et al, 1988). In both cases the flow was attached but did not exhibit fore and aft symmetry. Wu and Lee presented experimental data and mathematical calculations using the FIDAP computational fluid dynamics software program for the free settling of solid and porous ellipsoids of revolution for Reynolds numbers in the range 0.1–40 (R.M. Wu, Lee, 2001). For a solid ellipsoid of revolution of aspect ratio 0.7 with the major axis aligned parallel to the flow, the upstream and downstream streamlines were symmetrical at a Reynolds number of 0.1. At a Reynolds number of 40, recirculating eddies were visible on the downstream side.

The flow around elliptic cylinders is more general geometrical configurations than the canonical circular cylinder and provides a richer flow behavior characteristic of typical engineering flow configurations. For these cylinders, changes in eccentricity allow for shapes ranging from that

of a circular cylinder to a flat plate. There have been a few numerical simulations of flows over elliptic cylinders. Notable among these are those by Lugt and Haussling (Lugt and Haussling,1972, 1974) and Blodgett (Blodgett,1989). Lugt and Haussling have studied the flow over thin ellipses at various angles-of-attack for low Reynolds numbers (Lugt and Haussling,1972) and also the details of start-up over elliptic cylinders at 45º angle-of-attack (Lugt and Haussling,1974). Blodgett (Blodgett,1989) has performed a systematic study of two-dimensional (2D) flow over cylinders with various eccentricities and angles-of attack at Reynolds number ranging up to 1000. The above studies are limited to 2D simulations and are based on the vorticity-streamfunction formulation of the Navier–Stokes equations. In the past decade, direct numerical simulation of 3D flows at low to moderate Reynolds number have become possible and have primarily utilized spectral methods for spatial discretization. Spectral methods provide exponential accuracy through their global approximation (Canuto et al,1988) but their application has been generally limited to simple geometries. Spectral element (Patera,1984) and spectral multidomain (Street, and Macaraeg,1989) methods have been developed to handle problems in complex geometries and have become quite popular in recent years. These methods provide great flexibility in handling a broad range of geometric configurations but are computationally expensive and relatively difficult to implement. For the relatively simpler class of geometries like elliptic cylinders, prolate/oblate spheroids, and Juo-kowski airfoils, more specialized spectral methods based on a single domain and body-fitted orthogonal grid would be expected to perform efficiently and are the method of choice. The justification for developing efficient but specialized methods for these shapes come from recognizing the fact that these shapes encompass a wide range of configurations which are of practical as well as fundamental importance.

Characteristic regimes of flow past a circular cylinder

Recently Zdravkovich (Zdravkovich,1997), in an excellent monograph, has compiled almost all the experimental, analytical and numerical simulation data on flow past cylinders, available since 1938 and systematically classified this challenging flow phenomenon into five different flow regimes based on the Reynolds number. the first few regimes designated by Zdravkovich as (1) creeping laminar state (L1) of flow ($0 < Re < 4$), (2) laminar flow (L2) with steady separation ($4 < Re < 48$) forming a symmetric contra-rotating pair of vortices in the near wake, (3) laminar flow (L3) with periodic vortex shedding ($48 < Re < 180$) and finally (4) part of the transition-in-wake (TrW) regime ($180 < Re < 400$) when the three-dimensional instabilities lead to the formation of streamwise vortex structure. The wake of a fixed circular cylinder exhibits a large variety of complex phenomena stemming from the diverse instabilities growing in the near wake. The classification of these phenomena was primarily based on experimental measurements and therefore the limits describing the transition between the different regimes were sometimes not exactly established. However a rather clear classification relying either on the evolution of the Strouhal number (Chen,1987) or on the base pressure coefficient curve (Zdravkovich,1997) is nowadays available.According to these classifications, the following regimes can be highlighted: for $Re \leq 49$,

two stationary recirculation zones attached to the cylinder wall can be observed; then for 49 ≤ Re≤190, the wake is still laminar and consists of two periodic staggered rows of vortices forming the well-known Von Ka´rma´n streets, the vortices of each row being shed alternately from either side of the cylinder. For greater Reynolds numbers, the wake becomes three-dimensional (for 190 ≤ Re ≤ 260) and progressively turbulent. This regime is followed by the shear-layer transition (Re ≥1200) where the separating shear layers become unstable and finally by the boundary-layer transition (Re of order 10^5) which is associated to the drag crisis, i.e. a dramatic decrease of the drag coefficient. Over all these regimes, the flow exhibits a certain periodicity which is known as the Strouhal frequency, denoted by f_S. When a periodic vortex street is well established, this frequency corresponds to that of the vortex shedding frequency; in other cases where the Von Ka´rma´n streets are not clearly visible, the frequency can be defined as the one of the fluctuations of the streamwise velocity component for example.

The latest studies on the numerical simulation of flow past a circular cylinder

Rajani et al (Rajani et al, 2009) worked on the analysis of two- and three-dimensional flow past a circular cylinder in different laminar flow regimes. In this simulation, an implicit pressure-based finite volume method was used for time-accurate computation of incompressible flow using second order accurate convective flux discretisation schemes. The complex three dimensional flow structure of the cylinder wake is also reasonably captured by the present prediction procedure.

David and Hector (David and Hector, 2009) investigated flow separation behind two-dimensional ellipses with aspect ratios ranging from 0, a flat plate, to 1, a circular cylinder for Reynolds numbers less than 10 using both a cellular automata model and a commercial computational fluid dynamics software program. Fluctuations in the values of the stream function for laminar flow behind the ellipses were found at combinations of Reynolds number and aspect ratio near the critical values for separation.

Antoine et al (Antoine et al, 2009) presented numerical simulation for the flow past a circular cylinder which is able to oscillate transversely to the incident stream for a fixed Reynolds number equal to 100. The 2D Navier–Stokes equations were solved by a finite volume method with an industrial CFD code in which a coupling procedure has been implemented in order to obtain the cylinder displacement.

Numerical simulation of the governing equation

The flow field was governed by the Navier–Stokes equations, which read for a Newtonian incompressible fluid:

$$\begin{cases} div u = 0 \\ \dfrac{\partial u}{\partial t} + div(u \otimes u) = -\dfrac{1}{\rho}\nabla p + \nu \Delta u \end{cases} \quad \ldots (1)$$

where $u = (u\ v)^T$ is the velocity vector with u and v being respectively the streamwise and transverse velocity components, p is the pressure, ρ and ν are the fluid density and kinematic viscosity. As the Reynolds number does not rise above 190, the flow is assumed to be laminar and

two-dimensional according to the description of the flow regimes given by Williamson (Williamson, 1997) for this range of Reynolds numbers. The Navier–Stokes equations were discretized using the finite volume technique, i.e. integral form of the conservation equations were solved on control volumes which form a partition of the computational domain (Ferziger and Peric, 1996). Surface and volume integral approximations require the values of variables at locations other than the computational nodes. Indeed, the integrand involves the product of several variables (convective fluxes) or variable gradients at those locations (diffusive fluxes). The pressure field was first predicted, and then corrected by several iterations so that the Poisson equation for pressure and the momentum conservation equations for velocity were satisfied. Once Eq. (1) had been discretized and the pressure–velocity decoupling had been realized, the problem was represented by a matrix system composed of the cell-centered unknowns which has to be inverted. The resolution is performed with the pre-conditioned conjugate gradient method and provides the velocity components u and v, and the pressure p.

Fluent Model

Because of the paucity of relevant experimental and analytical data, the FLUENT (FLUENT Flow Modeling Software, 2007) computational fluid dynamics software was employed as a tool to complement the model and improve the understanding of the flows. Visual examination of the contours of stream function computed by the steady state FLUENT model provided an unambiguous indication of whether or not the flow was attached. All the computations use an implicit pressure-based finite volume Navier–Stokes algorithm (RANS3D). A CFD models were simulated for the viscous flow past bodies changed from a circular cylinder to flat plate. The engineering system in this research consist of rectangular region of (50x40) cm as apart of the flow past cylinder of (1cm) radius in the center of the rectangular region. **Figure (1)** showed the grid of the engineering system. The assumptions for this model for flow of air were:

1. Constant viscosity of (1 Kg/m.s).
2. Constant pressure of (1 atm).
3. Constant density of (1 kg/m^3)

Results And Discussion

The implicit finite volume solver RANS3D developed for general unstructured grid preprocessed in GAMBIT 2.3.16 had been used in this work for two- dimensional computation of the problem. In case of L1, L2 and L3 regime, where the flow is steady, the present computations are limited to two-dimensional flow only. The wake of a fixed cylinder of unit diameter was investigated for three Reynolds numbers in the regimes ($0.1 \leq Re \leq 190$). Simulations are carried out until the convergence residual becomes smaller than 10^{-7}. The Reynolds numbers investigated are 10, 40 and 150, all below the Hopf bifurcation between the permanent and the periodic regime, and the wake was thus characterized by two recirculation zones attached to the rear cylinder wall.

Figures (3) and **(4)** showed for the present computation with no blockage flow separation and formation of a closed wake was observed to take place only beyond Re = 6.1. Measurement data show that for flow Reynolds number beyond approximately 5, the flow separates on the cylinder surface and the wake behind the cylinder consists of a pair of symmetric contra-rotating vortices on either side of the wake centre line. Further it was observed that as the flow Reynolds number increases, **Figures (3)** and **(4)** show that beyond a critical Reynolds number of about 49, the steady closed near wake becomes unstable and a transverse oscillation starts near the end of the wake. As the Re is increased further, the vortices are shed alternately from the upper and lower cylinder surface at a definite frequency depending on the Reynolds number. Zdravkovich (Zdravkovich,1997) had mentioned about the wide scatter of the reported values of this critical Reynolds number at which the near wake instability initiates even when the blockage is negligible. As for the circular cylinder there was only a single separation point on each side of the bluff body, although it was fixed in position. At low Reynolds numbers the wake resembles the typical Ka´rma´n wake of a circular cylinder. As the Reynolds number was increased the wake rapidly evolved spatially downstream to two sets of positive and negative vortices distributed on either side of the wake centre line. The two dimensional wake was stated for a sequence of elliptical bodies with the circular cylinder and flat plate as limiting cases. Interestingly, the characteristic Ka´rma´n wake was displaced downstream by a wake consisting of two sets of vortices offset from the wake centre line, even at quite low Reynolds numbers, as the body geometry tends towards that of a normal flat plate.

Figure (3) showed the effect of eccentricity (aspect ratio) and Reynolds number on the static pressure contours. **Figure (3)** showed that the flow separates more largely on the cylinder surface and the wake behind the cylinder which consists of a pair of symmetric contra-rotating vortices on either side of the wake centre line will be larger when the aspect ratio increased from (0-1.3), this means that the geometry of the body effect positively on the flow separation and back flow in the wake region. The region of the lowest pressure decreases with increasing of Reynolds number until (Re=150) the flow will be separated.

Figure (4) showed the effect of eccentricity (aspect ratio) and Reynolds number on the contours of velocity magnitude. **Figure (4)** showed that the wake region and the back flow increased with increasing aspect ratio and will be more separated with increasing Reynolds number.

Figure (5) showed the effect of eccentricity (aspect ratio) and Reynolds number on the streamlines of the static pressure. **Figure (5)** showed that the curve of the pressure gradient with distance stretched horizontally with increasing aspect ratio. This means that the region of the back flow will be increased. At (Re≥150) the pressure gradient will be unstable behind the body.

Figure (6) showed the effect of eccentricity (aspect ratio) and Reynolds number on the streamlines of the velocity. **Figure (6)** showed that the velocity gradient curve for (aspect ratio≥0) will be oscillated behind the body with increasing Reynolds number because of the maximizing the oscillation of the back flow region.

This study confirms that two possible flow structures exist and shows that small changes in ellipticity (aspect ratio) can cause a sudden switch in state.

Comparing model results to other models

Comparisons with the published references show excellent agreement in detecting the drag, the lift, Strouhal number of the unbounded cylinder for different Reynolds numbers considered in this study. Some of the important variables of engineering interest for flow past cylinder with vortex shedding are the mean drag coefficient, and the Strouhal frequency of the lift coefficient. **Figure (2)** shows the variation of mean drag coefficient – its pressure and friction components and the Strouhal number with varying flow Reynolds number. For the mean drag coefficient, kink is observed in the present computation result at critical Reynolds number of about (49) when vortex shedding starts. However, the overall agreement between the present computation and the compiled data of Zdravkovich (Zdravkovich, 1997) is reasonably good. In case of Strouhal frequency of the lift coefficient, the present computation agrees reasonably well with measurement data of Norberg (Norberg,1993) only up to about Re=150 beyond which the two-dimensional flow computation over predicts the Strouhal number.

Conclusions

The wake structure behind a circular cylinder has been computed for two-dimensional flow, using second order accurate implicit finite volume Navier–Stokes solver RANS3D. Computations have been carried out for Reynolds numbers between 0.1 and 190 covering three different characteristic regimes classified by Zdravkovich (Zdravkovich, 1997) creeping flow (L1), steady closed near wake (L2) and the laminar vortex shedding regime(L3). Major physical features of the flow in different regimes are captured by the present computation procedure reasonably well. In the L1 and L2 regimes, reasonably good agreement is obtained between the two-dimensional computation results and the corresponding measurement data for the shape and strength of the steady wake recirculation zone including the separation location.

FLUENT models clearly demonstrate that the overall agreement between the present computation and the compiled data of Zdravkovich (Zdravkovich, 1997) is reasonably good. In case of Strouhal frequency of the lift coefficient, the present computation agrees reasonably well with measurement data of Norberg (Norberg, 1993) only up to about Re=150 beyond which the two-dimensional flow computation over predicts the Strouhal number. The computed critical Reynolds numbers for separation behind a flat plate and a cylinder are in close agreement with extrapolations made from experimental observations. It may provide valuable insight into how flow at such low Reynolds numbers occurs in the natural world. Steady state mathematical models of laminar flow are even more idealized.

References

[1 M. Coutanceau, R. Bouard, Experimental determination of the main features of the viscous flow in the wake of a circular cylinder in uniform translation. Part 1, steady flow, J. Fluid Mech. 79 (Pt. 2) (1977) 231–256.

D. Li, The small flow becomes main stream, Microfluidics Nanofluidics1 (1) (2004)1.

V. Streeter, Handbook of Fluid Dynamics, McGraw-Hill, New York, 1961.

H. Schlichting, Boundary-Layer Theory, McGraw-Hill, New York, 1979.

S. Taneda, Experimental investigation of the wakes behind cylinders and plates at low Reynolds numbers, J. Phys. Soc. Jpn. 11 (3) (1956) 303–307.

S. Taneda, Standing Twin-Vortices Behind a Thin Flat Plate Normal to the Flow, Reports of Research Institute for Applied Mechanics, Kyushu University, vol. 54, 1968, pp. 155–163.

S. Dennis, G. Chang, Numerical solutions for steady flow past a circular cylinder at Reynolds numbers up to 100, J. Fluid Mech. 42 (Pt. 3) (1970) 471–489.

F. Nieuwstadt, H.B. Keller, Viscous flow past circular cylinders, Comput. Fluids 1 (1973) 59–71.

M. Van Dyke, An Album of Fluid Motion, Parabolic Press, Stanford, 1982.

K. Shintani, A. Umemura, A. Takano, Low-Reynolds-number flow past an elliptic cylinder, J. Fluid Mech. 136 (1983) 277–289.

Y. Nakayama, W.A. Woods, D.G. Clark, Visualized Flow: Fluid Motion in Basic and Engineering Situations Revealed by Flow Visualization, Pergamon, Oxford, 1988.

R.M. Wu, D.J. Lee, Hydrodynamic drag on non-spherical floc and free-settling test, Water Res. 35 (13) (2001) 3226–3234.

H. J. Lugt and H. J. Haussling, Naval Ship Research and Development Center Report 3748, Dept. of Navy, 1972 (unpublished).

H. J. Lugt and H. J. Haussling, *J. Fluid Mech.* **65**(4), 771 (1974).

K. E. J. Blodgett, M.S. thesis, Department of Aerospace Engineering and Engineering Mechanics, University of Cincinnati, 1989 (unpublished).

C. Canuto, M. Y. Hussaini, A. Quarteroni, and T. A. Zang, *Spectral Methods in Fluid Dynamics* (Springer-Verlag, New York, 1988).

A. T. Patera, *J. Comput. Phys.* **54,** 468 (1984).

C. L. Street, and M. Macaraeg, *Appl. Numer. Math.* **6,** 123 (1989).

M. Zdravkovich, Flow Around Circular Cylinders, vol. 1, Oxford Science Publication, 1997.

Chen S-S. Flow-induced vibration of circular cylindrical structures. Springer Verlag; 1987.

B.N. Rajani , A. Kandasamy , Sekhar M., Flow separation behind ellipses at Reynolds numbers less than 10, Applied Mathematical Modelling, 33 (2009) 1228–1247.

David S., Hector R. Bravo, Numerical simulation of laminar flow past a circular cylinder, Applied Mathematical Modelling, 33 (2009) 1633–1643.

Antoine P., J. Sigrist , Aziz H., Numerical simulation of an oscillating cylinder in a cross-flow at low Reynolds number: Forced and free oscillations, Computers & Fluids, 38 (2009) ,80–100.

Williamson C-H-K. Advances in our understanding of vortex dynamics in bluff body wakes. J Wind Eng Ind Aerodyn 1997:3–32.

Ferziger J-H, Peric´ M. Computational methods for fluid dynamics. Springer Verlag; 1996.

FLUENT Flow Modeling Software, Fluent Inc., Lebanon, NH, 2007.

C. Norberg, Pressure forces on a circular cylinder in cross flow, Springer-Verlag, Berlin, 1993, pp. 275–278.

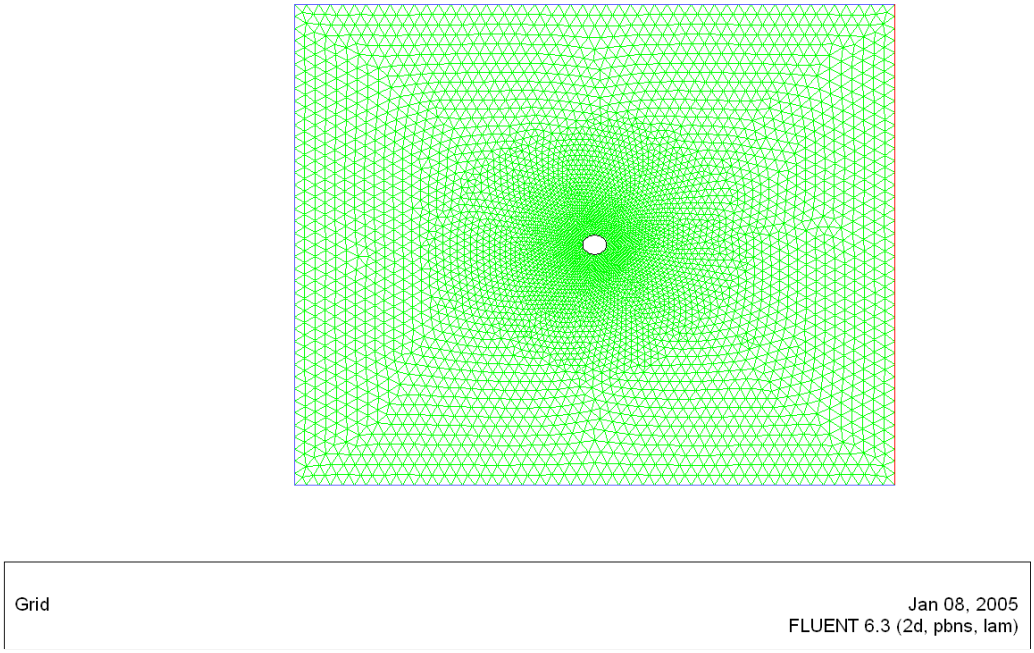

Figure (1): The grid of the engineering system.

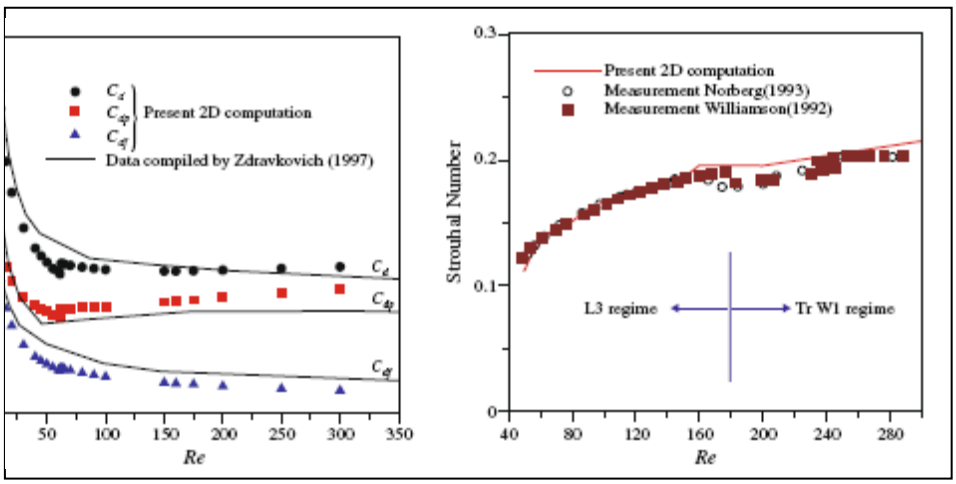

(a) Mean Drag (b) Strouhal number

Figure (2): Variation of mean drag coefficient (comparison with data of Zdravkovich) , Strouhal number with Re(comparison with measurement data of Norberg, Williamson) .

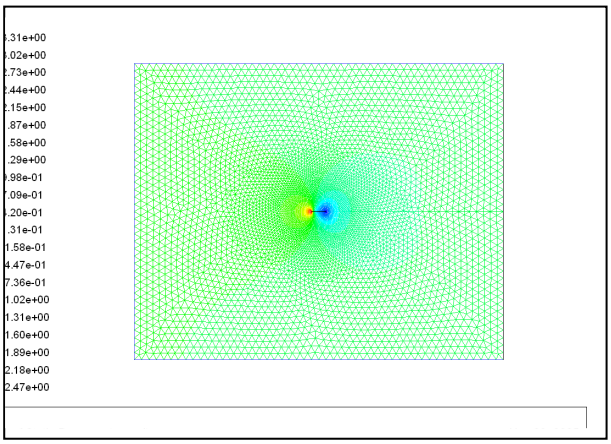

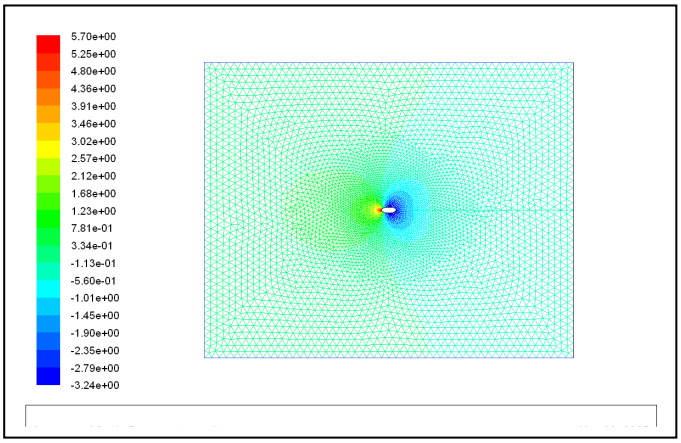

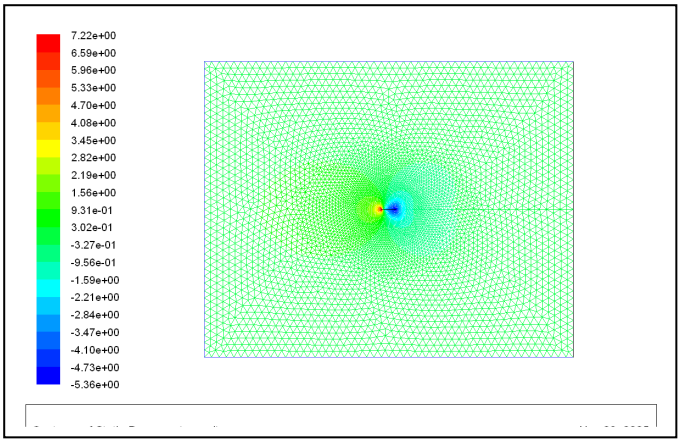

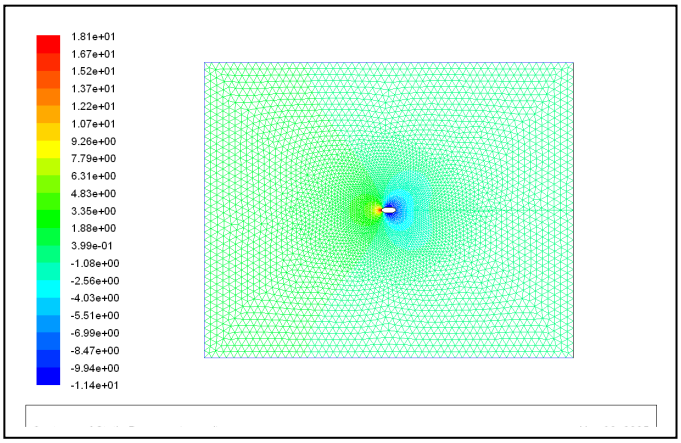

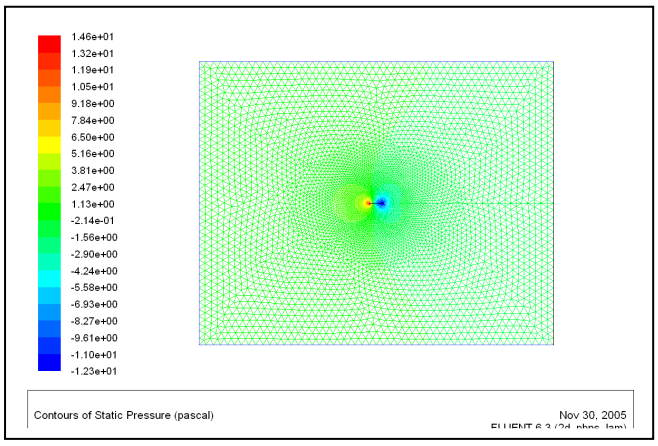

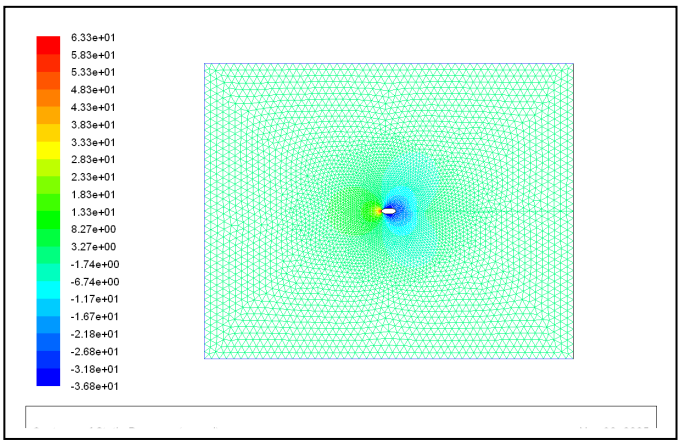

Figure (3): Details of the static pressure contours (Pascal) at Re = 10, 40, 150, (left) for Aspect Ratio=0 and (right) for Aspect Ratio=0.4.

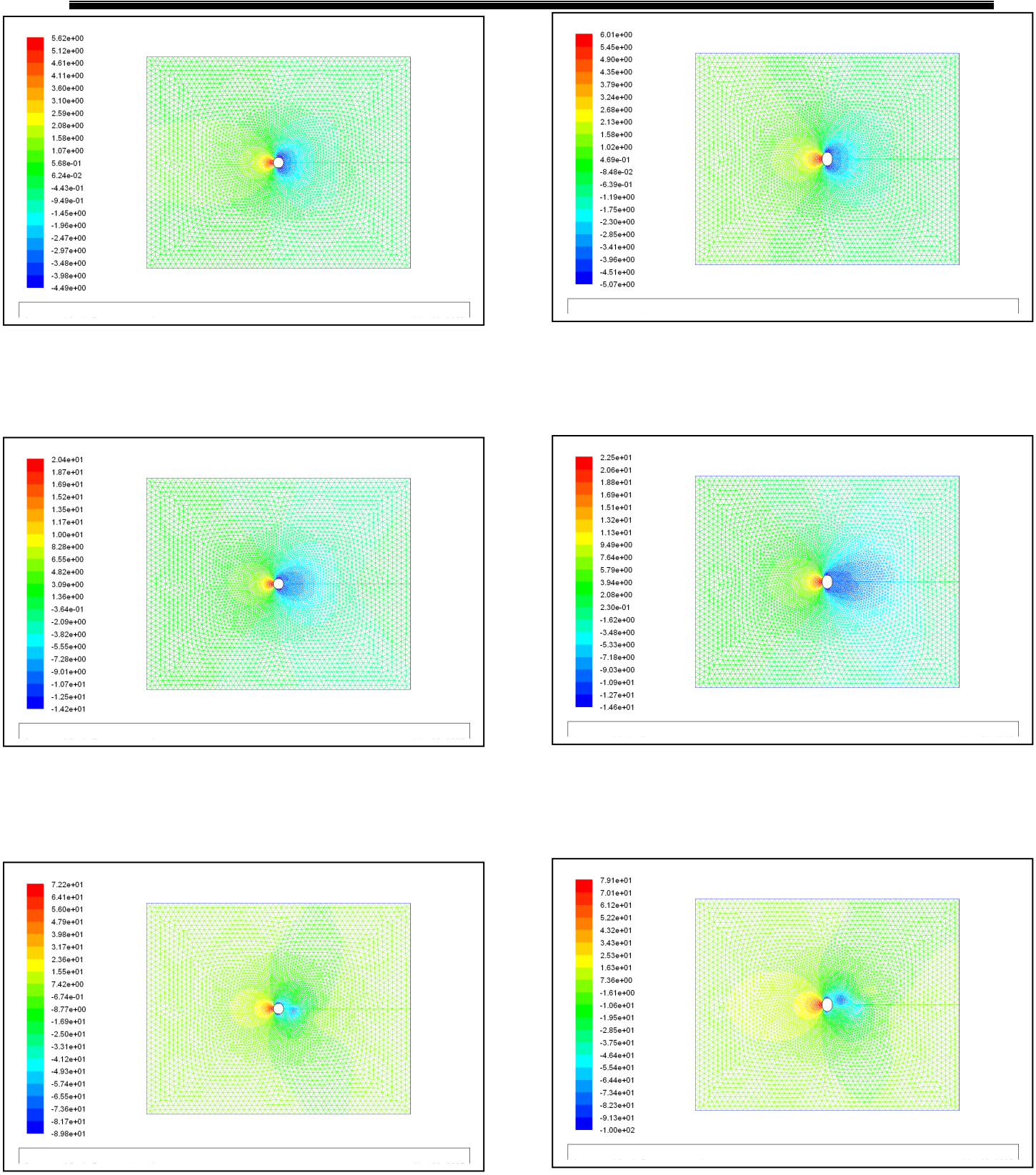

Figure (3): Details of the static pressure contours (Pascal) at Re = 10, 40, 150, (left) for Aspect Ratio=1and (right) for Aspect Ratio=1.3(continued).

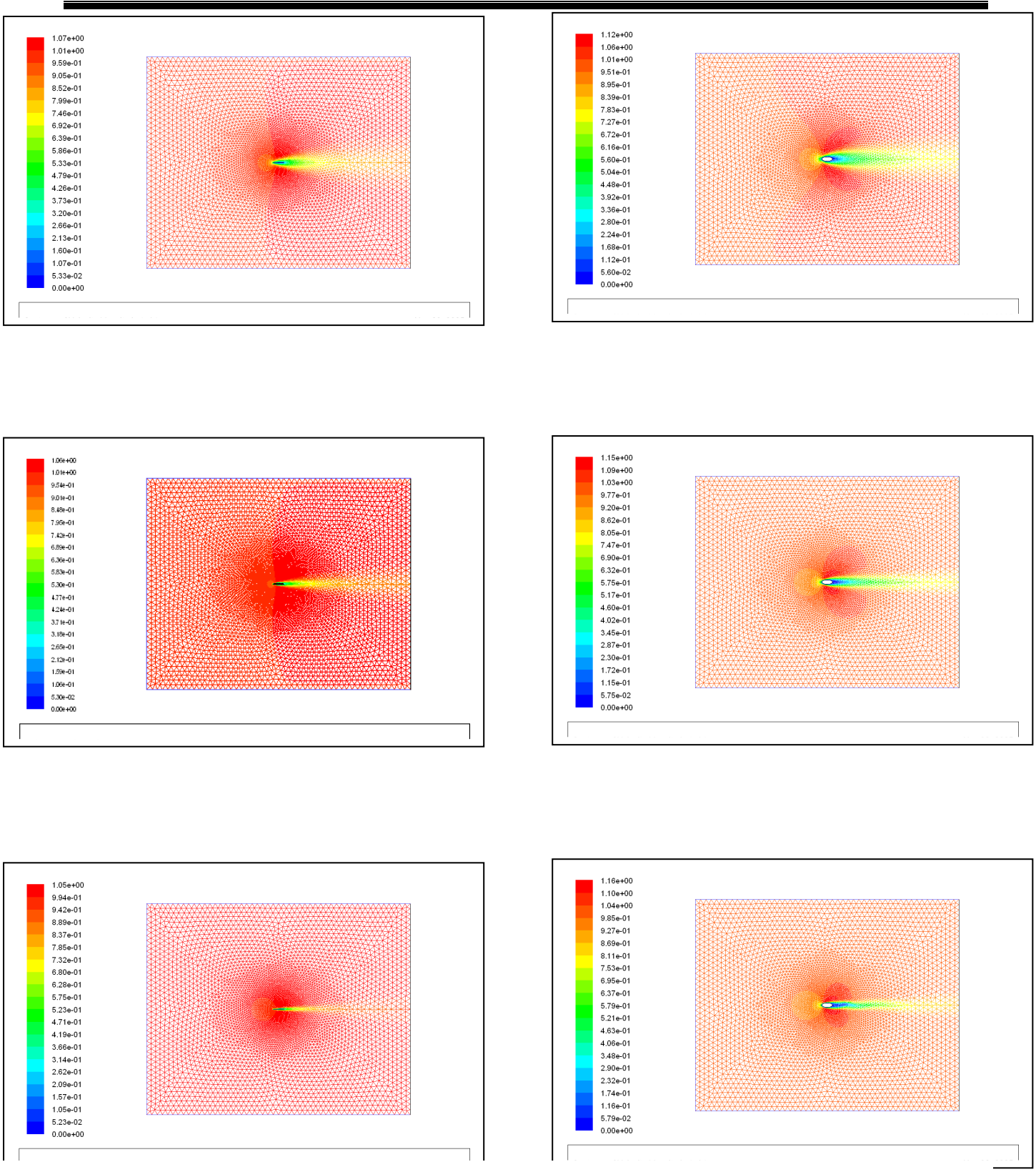

Figure (3): Contours of velocity magnitude (m/s) at Re = 10, 40, 150, (left) for Aspect Ratio=0 and (right) for Aspect Ratio=0.4.

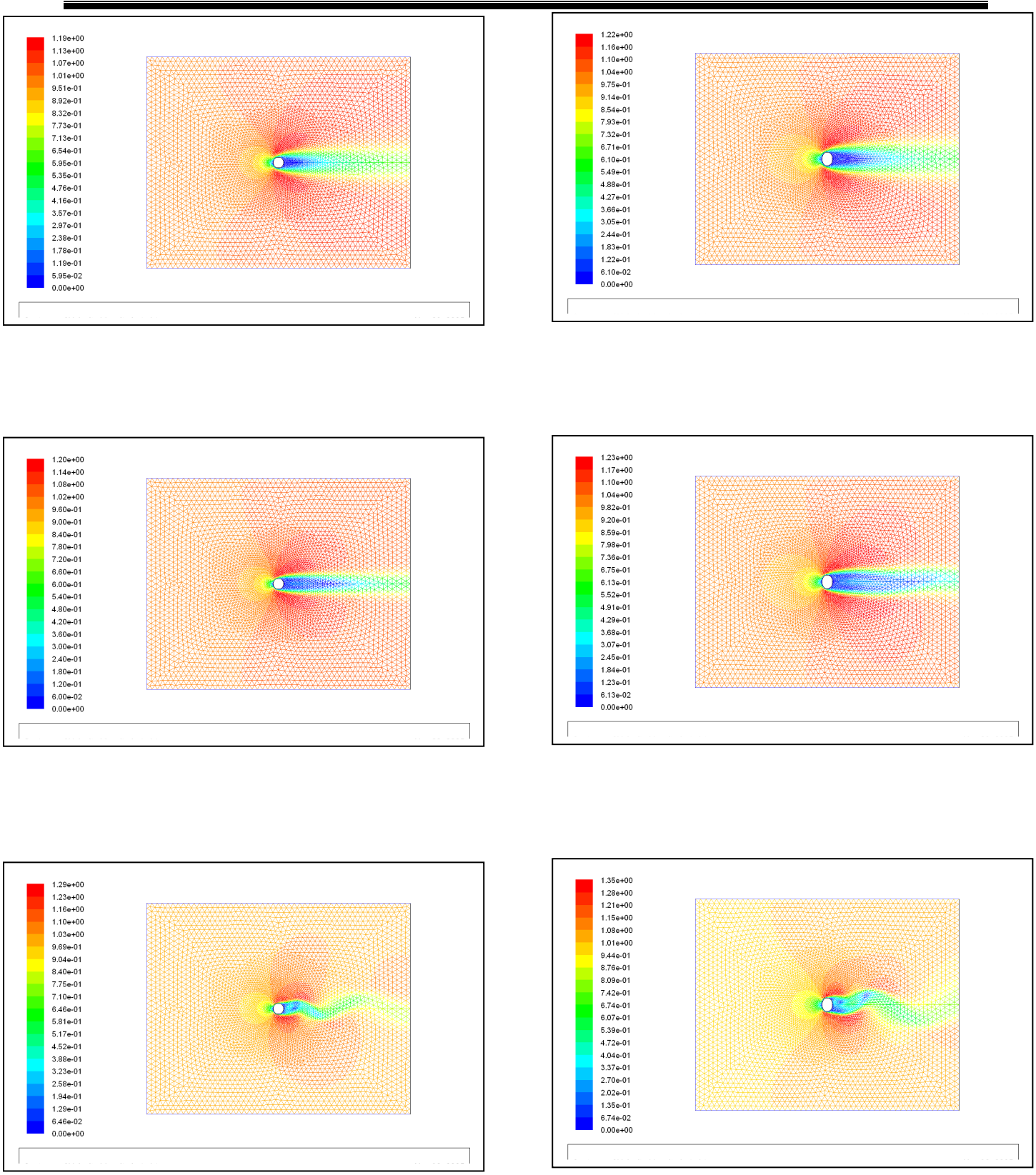

Figure (4): Contours of velocity magnitude (m/s) at Re = 10, 40, 150, (left) for Aspect Ratio=1 and (right) for Aspect Ratio=1.3(continued).

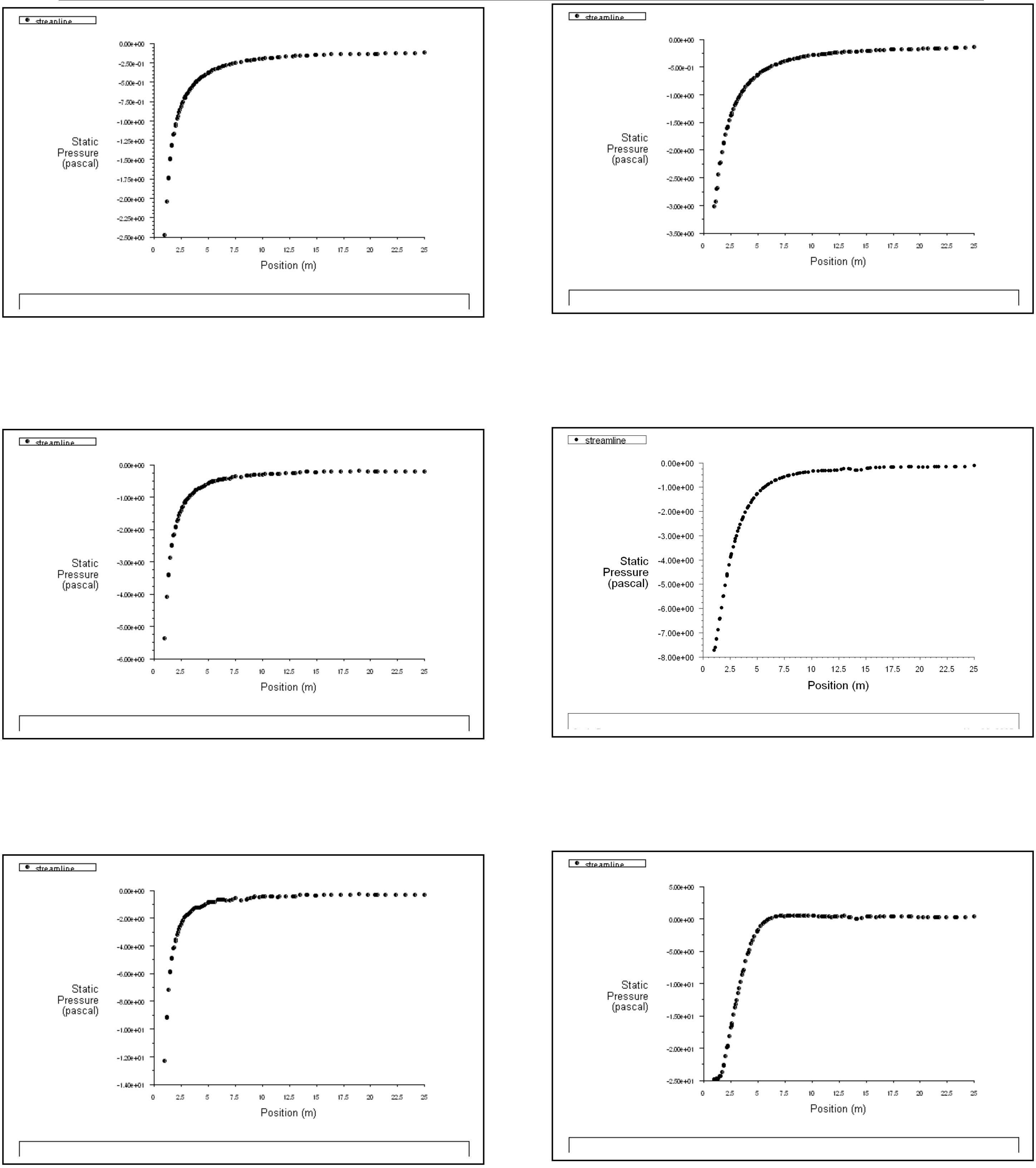

Figure (5): Streamlines of the static pressure versus the downstream distance after the cylinder wall at Re = 10, 40, 150, (left) for Aspect Ratio=0 and (right) for Aspect Ratio=0.4.

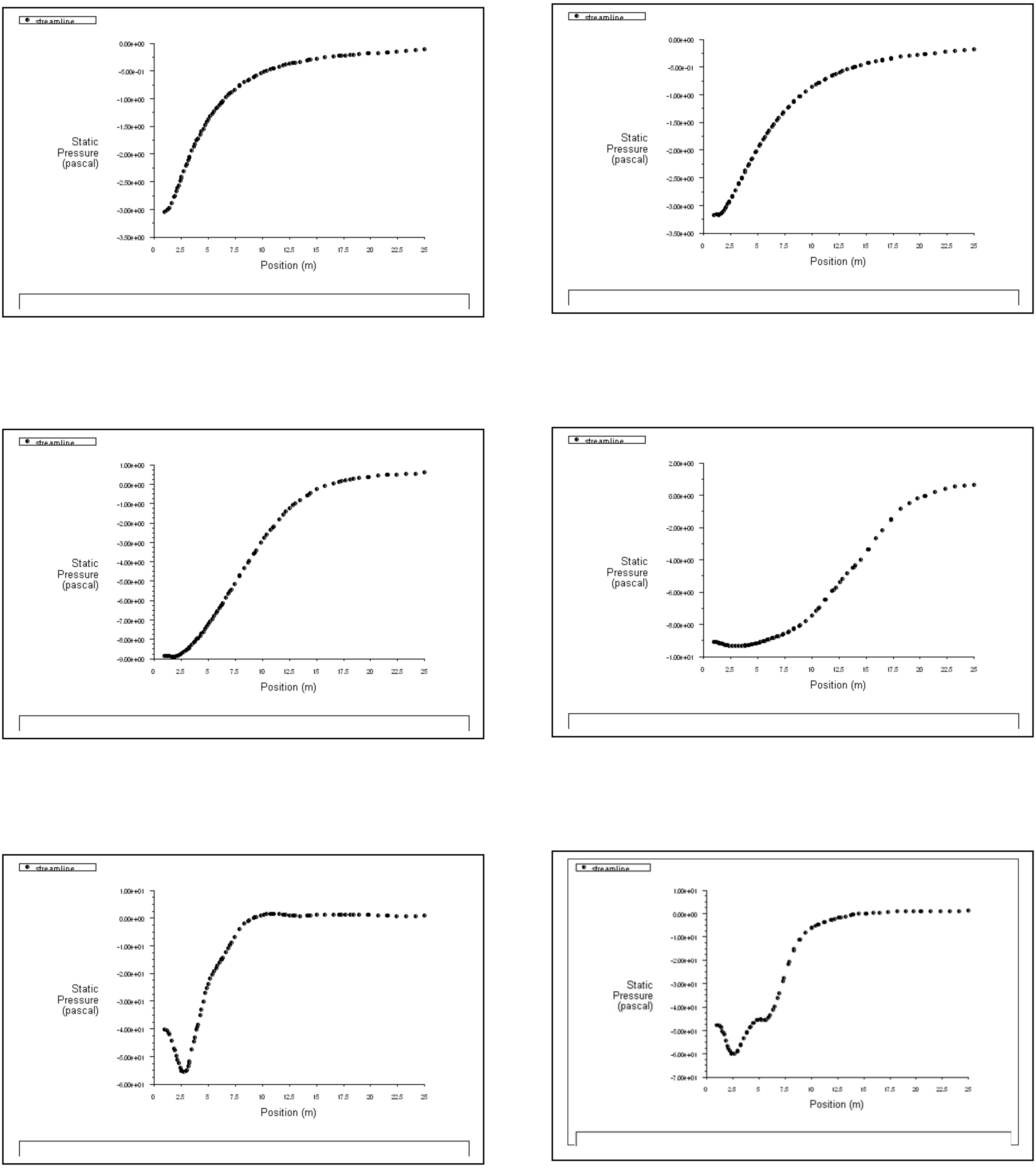

Figure (5): Streamlines of the static pressure versus the downstream distance after the cylinder wall at Re = 10, 40, 150, (left) for Aspect Ratio=0 and (right) for Aspect Ratio=0.4.

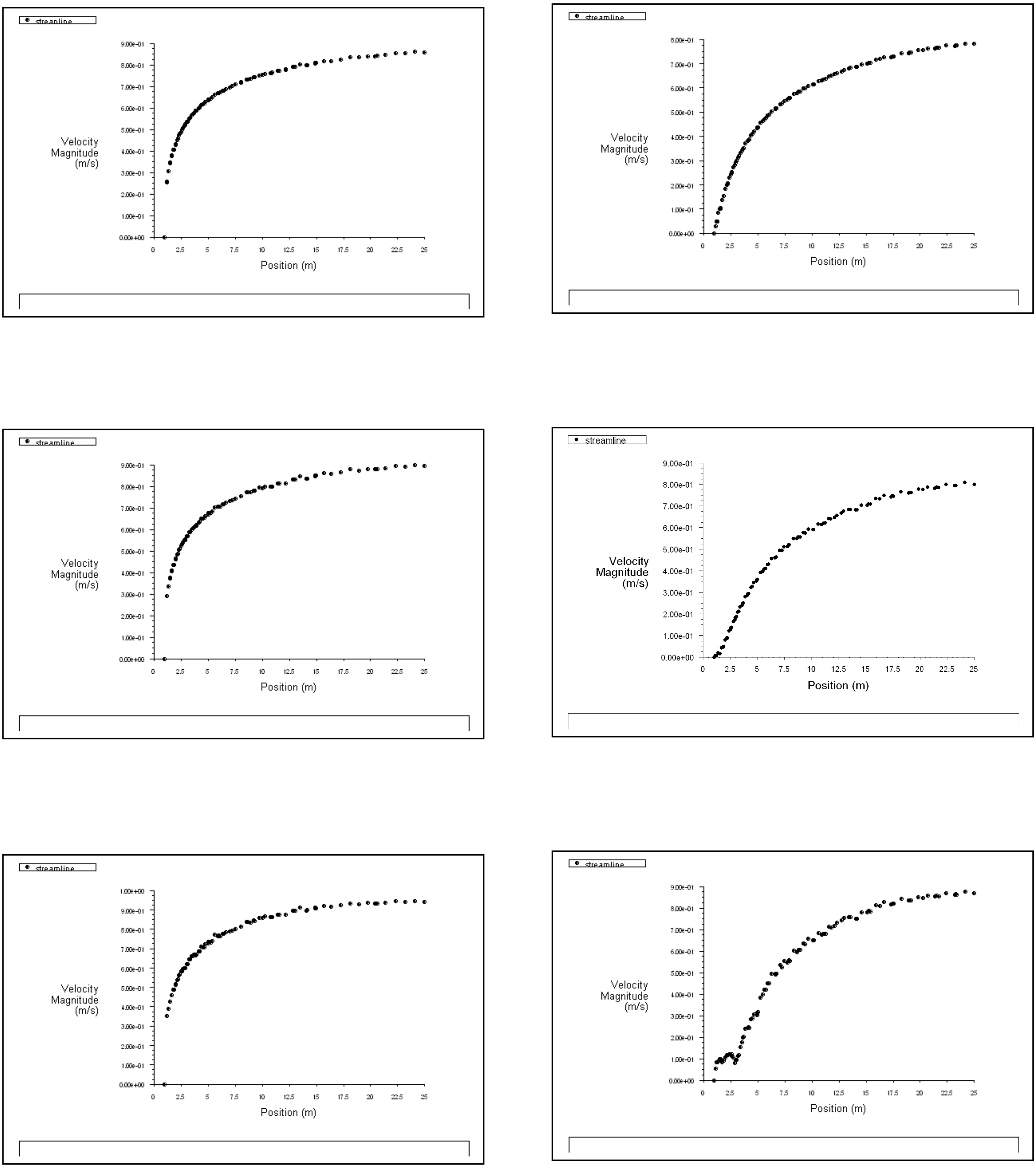

Figure (6): streamlines of the velocity versus the downstream distance after the cylinder wall at Re = 10, 40, and 150, (left) for Aspect Ratio=1 and (right) for Aspect Ratio=1.3.

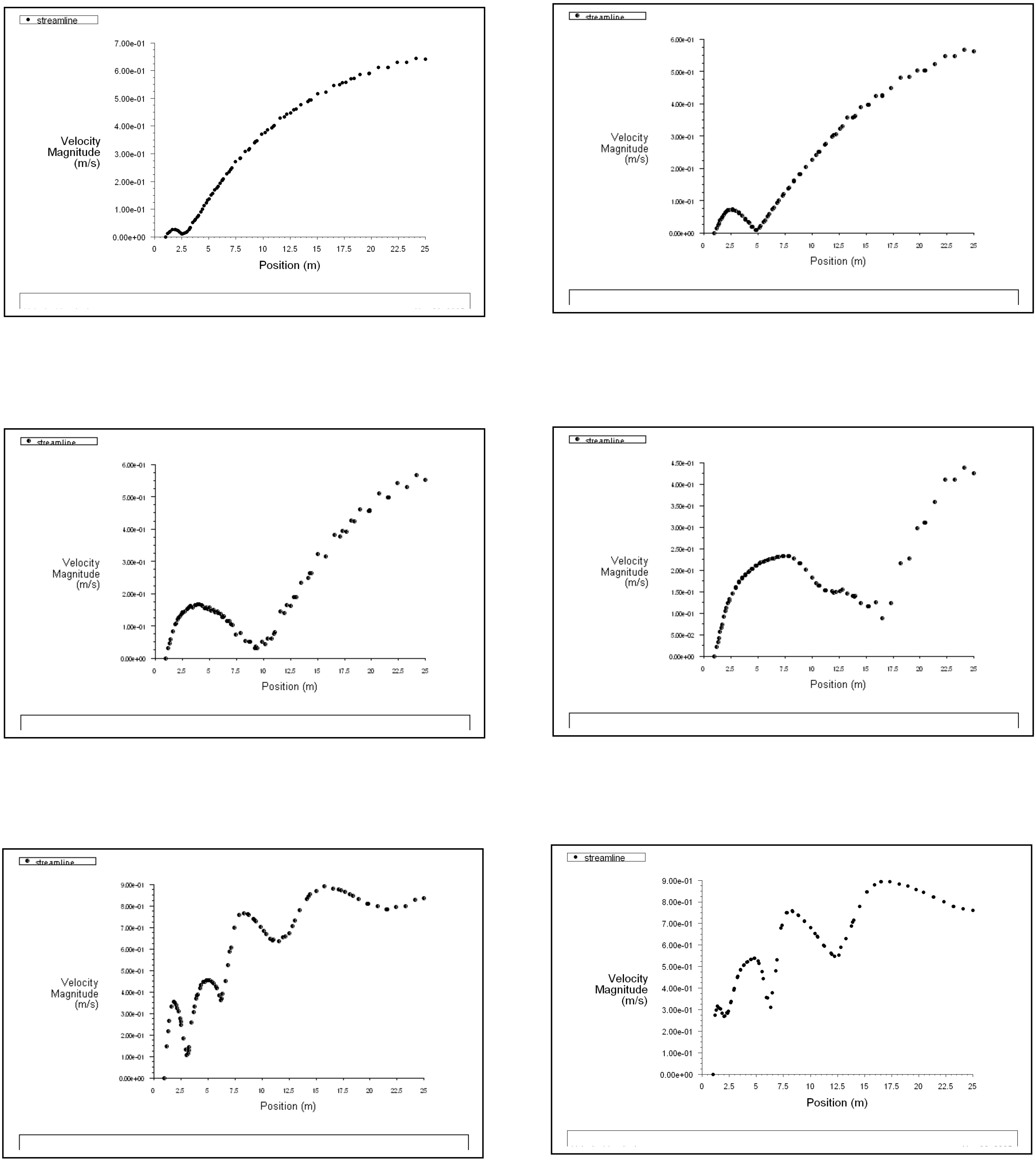

Figure (6): streamlines of the velocity versus the downstream distance after the cylinder wall at Re = 10, 40, 150, (left) for Aspect Ratio=1 and (right) for Aspect Ratio=1.3(continued).

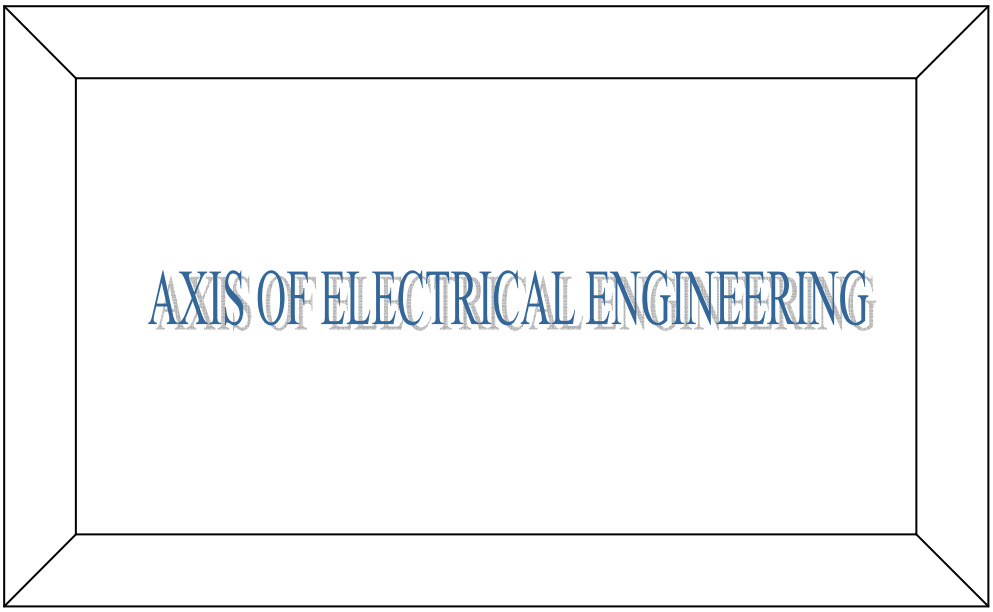
AXIS OF ELECTRICAL ENGINEERING

IMPROVING TRANSIENT STABILITY IN CASE OF FAULTS IN HADITHA - QAIM LINE

Dr. Samir S. Mustafa
Technical Institute / Kirkuk

Abstract

Iraqi National Super Grid suffers from out of synchronism of the system due to short circuit in the lines. The main goal of this work is to study the effect of optimum generation and reconfiguration of some transmission paths on transient stability improvement for Iraqi Network in case of short circuit in Haditha-Qaim line because it is one of the wrest lines. A programmable package build under Matlab5.3 was used to determine synchronous machines rotor angles as an indicator of transient stability. Sad Al-Mosul, Haditha and Nasiriya power plant were chosen to notice the situation of stability.
Keywords- Power Losses, Transient Stability, Stability, Reconfiguration.

تحسين الاستقرارية العابرة في حالة الخلل في خط حديثة – ألقائم

د . سمير سعدون مصطفى
أستاذ مساعد
ألمعهد ألتقني / كركوك

الخلاصة

تعاني شبكة الضغط الفائق في العراق من مشكلة خروج المنظومة عن التزامن وذلك عند حدوث دائرة قصر في احد خطوط الشبكة. يهدف هذا البحث إلى دراسة تأثير التوليد الأمثل وتأثير إعادة تشكيل بعض مسارات الخطوط في تحسين الاستقرارية العابرة في شبكة الضغط الفائق وذلك عند حدوث دائرة قصر في خط حديثة – القائم لأنه يعتبر أحد أضعف الخطوط في المنظومة. تم استخدام برنامج جاهز بلغة Matlab5.3 لحساب زوايا دوار المكائن التزامنية كمؤشر لحالة الاستقرارية.تم اختيار محطات توليد سد الموصل، حديثة و الناصرية لملاحظة أستقرارية المنظومة.

Introduction

Power System Stability

The importance of power system stability is increasingly becoming one of the most limiting factors for system performance. By the stability of a power systems we mean the ability of the system to remain in operating equilibrium, or synchronism, while disturbances occur on the system(Kundur2004). There are three types of stability namely, steady-stat, dynamic, and transient stability.

1) Steady-State stability: refer to the stability of a power system subject to small and gradual changes in load and the system remains stable with conventional excitation and governor controls.